Progress in Fractional Differentiation and Applications
An International Journal

http://dx.doi.org/10.18576/pfda/090402

Two New Quadratic Scheme for Fractional Differential Equation with World Population Growth Model

Pawan Kumar Shaw[1], *Sunil Kumar*[2,3,4,5,*], *Shaher Momani*[3,6] *and Samir Hadid*[3,7]

[1] Centre for Data Science, ITER, Siksha O Anusandhan (Deemed to be University), Bhubaneswar, India
[2] Department of Mathematics, National Institute of Technology, Jamshedpur, 831014, Jharkhand, India
[3] Nonlinear Dynamics Research Center (NDRC), Ajman University, Ajman, UAE
[4] Department of Mathematics, College of Science, King Saud University, P.O. Box 2455, Riyadh 11451, Saudi Arabia
[5] Department of Mathematics, University Centre for Research and Development, Chandigarh University, Gharuan, Mohali, Punjab, India
[6] Department of Mathematics, Faculty of Science, University of Jordan, Amman 11942, Jordan
[7] Department of Mathematics and Sciences, College of Humanities and Sciences, Ajman University, Ajman, UAE

Received: 4 Jan. 2022, Revised: 26 Feb. 2022, Accepted: 28 Feb. 2022
Published online: 1 Oct. 2023

Abstract: In this paper, we proposed two quadratic convergence numerical technique which are very accurate and fast for finding the approximate solution of an initial value problem (IVP) of the linear as well as non-linear fractional differential equations (FDEs) of arbitrary order ρ, where $0 < \rho \leq 1$. Here, our fractional derivative are taken in the Caputo sense. In this suggested work, we provides the numerical solution which is comparatively faster and accurate than the Euler method (EM), Improved Euler method (IEM), and many other linear, quadratic convergence methods. Also, here we have been found the numerical solution without the help of any kind of linearisation, perturbations or any other assumptions. Illustrated example shows the numerical comparisons in sense of efficiency and accuracy between the our proposed scheme and the exact solution, Euler method and the Improved Euler method of the IVP of FDEs. Our both the proposed scheme Ralston's method and Ralston's method of minimum local error bound has quadratic convergence which is more accurate and faster than the Euler method and Improved Euler method, while Improved Euler has also quadratic convergence rate.

Keywords: Initial value problem, fractional world population growth model, fractional midpoint method, fractional Ralston's method, fractional Ralston's method with minimum local error bound.

1 Introduction

The word fractional calculus (FC) indicates the generalization of differentiation and integration of arbitrary order which is not necessarily the integer order. This fractional differential and integral have attracted many research field of engineering, science, economics and many more. Some interesting research areas of fractional calculus can found in viscoelastic theory, control theory, chaotic systems, electromagnetic waves, electronic chemicals fractal theory, nonlinear dynamical systems and many more [1,2,3,4,5]. Nevertheless, the concept of fractional calculus arose when L'Hopital questioned Leibniz about the differentiation of half-order in the year 1695. This inquiry marked the beginning of the exploration into fractional calculus and its fascinating properties. In his reply, Leibniz wrote to L'Hopital dated 30 Sept, 1695, "This is an apparent Paradox from which, one day, useful consequences will be drawn" [6,7,8]. Fractional calculus, after its initial inquiry by L'Hopital and Leibniz in 1695, has undergone further generalization by several, mathematicians and eminent researchers. In recent decades, the study of IVP of FDEs has garnered significant importance in comprehending various physical phenomena. Numerous researchers have contributed to establishing the existence and uniqueness conditions for IVPs of FDEs of arbitrary order [9,10,11].

* Corresponding author e-mail: skumar.math@nitjsr.ac.in

Now a days, developing the exact and numerical solution of IVP of FDEs of arbitrary order becomes a popular and challenging research in the field of FDEs [12,13]. But a huge number of FDEs specially non-linear FDEs don't have exact solutions, so for that many author proposed the different numerical technique to find the approximate result of such IVP of FDEs. These method includes variational iteration method [14,15], homotopy perturbation scheme, homotopy analysis scheme [16], Adomain decomposition scheme [17,18,19], fractional differential transform scheme [20,21], fractional finite difference scheme [22], fractional Adams scheme [23], spectral collocation scheme [24], and many others. It is also found from the literature [17,18,19,20,21,22,23,24], some numerical scheme have some drawback which enhance the derivative of Riemann Liouville. In our work, we provide some novel scheme to remove such drawback.

In recent research, Kumar et al. introduced several numerical schemes to investigate the numerical solution of IVP associated with FDEs [25,26,27]. One of these methods is the midpoint method, which exhibits quadratic convergence rate. Additionally, Tong et al. [28] introduced an improved Euler method with a quadratic convergence rate. Apart from these, from the last few decades many researchers proposed the several iterative numerical technique [29,30]. Here, in our suggested work, we proposed the two new explicit numerical technique, one is Ralston method (RM)[31] and another is Ralston method two stage with minimum local error bound (RME) [32,33,34] which is conventionally known as Ralston method 1 and Ralston method 2. The suggested method has better approximation results in comparison to fractional EM, fractional IEM and fractional midpoint method (MPM) for obtaining the numerical solution of FDEs which is of the form,

$$ {}^{C}\mathscr{D}^{\rho}_{a^+}u = F(t,u), \text{ together with } u(a) = u_0, \text{ and } t \in [a, t_{end}]. \tag{1}$$

Here, $0 < \rho \leq 1$ and ${}^{C}\mathscr{D}^{\rho}_{a^+}$ represent the fractional order derivative in Caputo sense.

In this paper, our main objective is to propose two novel and accurate method for approximating the solution of the IVP of FDEs (1). We aim to propose a method that can effectively handle FDEs and provide reliable results for various physical and engineering problems. For that, we explore the two new scheme of single step such as RM and RME. In the classical ODE, RME scheme was first proposed by Anthony Ralston in the year 1962 [32] and later one equivalent method was found which is similar as RME which is conventionally know as RM [31]. These two method is the type of Runge-Kutta second order method in which RME contains the minimum local error bound [32,35] compare to other RK2 method. With this fact, now a question arises: can we have such method in the IVP of FDEs ? This question motivate us to establish such accurate scheme for (1). Theses scheme encompasses the algorithm, convergence results, and numerical examples for both linear and non-linear cases. It demonstrates the method's accuracy, and versatility across various scenarios. These methods also known as the type of RK2 method and this is explicit "One-Step" method.

This paper is structured as in the following manner. In Section 2, we state and provide some necessary result, definition and properties of FDEs in both Riemann and Caputo derivative sense. In Section 3, we proposed our IVP of FDEs and our two suggested algorithm Ralston method and Ralston method two stage with minimum local error bound and also we prove the convergence of the suggested method and then the analysis of error of both scheme. In Section 4 , we gave four example in which the first one is our real world example of world population growth model and then next three one are the specific IVP of FDEs in linear as well as non-linear form which is estimated with figures and tables. In the final Section 5, we summarize and conclude our findings and contributions.

2 Preliminaries

In this section, we explore the basic of fractional differential and integral calculus, along with the Mittag-Leffler function. These concepts serve as natural generalizations of ordinary calculus and have wide applications in various scientific and engineering fields. We reference essential works such as [36,37,38,39,40,41,42,43,44,45,46,47] to provide comprehensive insights into these topics, enabling us to advance our understanding of FC and its practical applications.

Definition 1. The Riemann-Liouville fractional order integral, defined for a function $\eta \in (L_1[a,b],\mathbb{R})$ with an arbitrary order $\rho > 0$, can be expressed as:

$$I^{\rho}_{a+}\eta(\zeta) = \frac{1}{\Gamma(\rho)}\int_a^{\zeta}(\zeta - s)^{\rho-1}\eta(s)ds, \zeta > a,$$

and

$$I^{\rho}_{b-}\eta(\zeta) = \frac{1}{\Gamma(\rho)}\int_{\zeta}^{b}(s - \zeta)^{\rho-1}\eta(s)ds, \zeta < b.$$

These integrals are commonly referred to as the left and right Riemann-Liouville integrals, respectively.

Definition 2. The Riemann-Liouville fractional order derivative applies to a function $\eta \in (L_1[a,b],\mathbb{R})$ with an order $\rho > 0$ and is given by:

$$ {}^{RL}\mathscr{D}^{\rho}_{a+}\eta(\zeta) = \frac{1}{\Gamma(n-\rho)}\frac{d^n}{d\zeta^n}\int_a^{\zeta}(\zeta-s)^{n-\rho-1}\eta(s)ds,\ \zeta > a, $$

and

$$ {}^{RL}\mathscr{D}^{\rho}_{b-}\eta(\zeta) = \frac{(-1)^n}{\Gamma(n-\rho)}\frac{d^n}{d\zeta^n}\int_{\zeta}^{b}(s-\zeta)^{n-\rho-1}\eta(s)ds, \zeta < b. $$

These derivatives are referred as the left and right Riemann-Liouville derivatives, respectively. The value of n is integer satisfying $n-1 < \rho \le n$. In the specific case when $0 < \rho < 1$, the derivatives can be expressed as:

$$ {}^{RL}\mathscr{D}^{\rho}_{a+}\eta(\zeta) = \frac{1}{\Gamma(1-\rho)}\frac{d}{d\zeta}\int_a^{\zeta}(\zeta-s)^{-\rho}\eta(s)ds, \zeta > a, $$

and

$$ {}^{RL}\mathscr{D}^{\rho}_{b-}\eta(\zeta) = -\frac{1}{\Gamma(1-\rho)}\frac{d}{d\zeta}\int_{\zeta}^{b}(s-\zeta)^{-\rho}\eta(s)ds, \zeta < b. $$

Definition 3. The Caputo fractional order derivatives are applicable to a function $\eta \in (L_1[a,b],\mathbb{R})$ with an order $\rho > 0$, and they are defined as follows:

$$ {}^{C}\mathscr{D}^{\rho}_{a+}\eta(\zeta) = \frac{1}{\Gamma(n-\rho)}\int_a^{\zeta}(\zeta-s)^{n-\rho-1}\eta^n(s)ds,\ \zeta > a, $$

and

$$ {}^{C}\mathscr{D}^{\rho}_{b-}\eta(\zeta) = \frac{(-1)^n}{\Gamma(n-\rho)}\int_{\zeta}^{b}(s-\zeta)^{n-\rho-1}\eta^n(s)ds, \zeta < b. $$

These derivatives are known as the left Caputo and right Caputo fractional derivatives respectively, with $n = 1+[\rho]$. In the specific case of $0 < \rho < 1$, the derivatives can be expressed as:

$$ {}^{C}\mathscr{D}^{\rho}_{a+}\eta(\zeta) = \frac{1}{\Gamma(1-\rho)}\int_a^{\zeta}(\zeta-s)^{-\rho}\eta'(s)ds, \zeta > a, $$

and

$$ {}^{C}\mathscr{D}^{\rho}_{b-}\eta(\zeta) = -\frac{1}{\Gamma(1-\rho)}\int_{\zeta}^{b}(s-\zeta)^{-\rho}\eta'(s)ds, \zeta < b. $$

The connection between the fractional order derivatives in the Caputo and Riemann-Liouville sense is established by the following equations:

For the left-sided derivatives:

$$ {}^{C}\mathscr{D}^{\rho}_{a+}\eta(\zeta) = {}^{RL}\mathscr{D}^{\rho}_{a+}\eta(\zeta) - \sum_{k=0}^{n-1}\eta^{(k)}(a)\frac{(\zeta-a)^{k-\rho}}{\Gamma(k-\rho+1)}, $$

For the right-sided derivatives:

$$ {}^{C}\mathscr{D}^{\rho}_{b-}\eta(\zeta) = {}^{RL}\mathscr{D}^{\rho}_{b-}\eta(\zeta) - \sum_{k=0}^{n-1}\eta^{(k)}(b)\frac{(b-\zeta)^{k-\rho}}{\Gamma(k-\rho+1)}, $$

where $n = 1+[\rho]$.

Definition 4. The Mittag-Leffler function for the one and two parameter family are represented by

$$ E_{\rho}(\zeta) = \sum_{k=0}^{\infty}\frac{\zeta^k}{\Gamma(\rho k+1)}\ \ \zeta \in \mathbb{C};\ \rho > 0, $$

and

$$ E_{\rho,\gamma}(\zeta) = \sum_{k=0}^{\infty}\frac{\zeta^k}{\Gamma(\rho k+\gamma)}\ \ \zeta \in \mathbb{C};\ \rho,\gamma > 0, $$

respectively.

Lemma 1. If ρ and γ are both non-negative, and F is a function in the space $L_1[a,b]$, then the following identities hold:

$$I^{\rho}_{a^+} I^{\gamma}_{a^+} g = I^{\rho+\gamma}_{a^+} g, \;\; I^{\rho}_{b^-} I^{\gamma}_{b^-} F = I^{\rho+\gamma}_{b^-} F,$$

valid across the entire interval $[a,b]$. Furthermore, if $F(t)$ is a continuous function on $[a,b]$, or if $\rho+\gamma \geq 1$, then these identities are valid throughout $[a,b]$.

Lemma 2.[38] If ρ and γ are both positive such that there exists an integer m with $m \leq k$, and ρ and $\rho+\gamma$ lie within the interval $[m-1,m]$, and if g is a function in $C^k[a,b]$ for some $a<b$ and $k \in \mathbb{N}$, then the equality holds:

$${}^{C}\mathscr{D}^{\rho}_{a^+}\, {}^{C}\mathscr{D}^{\gamma}_{a^+} F = {}^{C}\mathscr{D}^{\rho+\gamma}_{a^+} F.$$

Theorem 1(Existence). [28] If the function $F(t,u)$ satisfies the condition $F(t_0,u(t_0))=0$ and is continuous on the region $D: 0 \leq t-t_0 \leq c,\ |u-u_0| \leq d$, then the FDE,

$${}^{C}\mathscr{D}^{\rho}_{a^+} u = F(t,u), \;\; \text{with } u(a)=u_0 \;\; \text{and, } t \in [a, t_{end}], \tag{2}$$

has at least one solution within the interval $0 \leq t-t_0 \leq L$, where L is the minimum value between c and $\frac{d}{M}$. Here, M represents the maximum value of ${}^{C}\mathscr{D}^{1-\rho}_{a^+} F(t,u)$ for all possible (t,u) in the real domain.

Theorem 2(Uniqueness). [28] In connection with Theorem 1, if the function $F_t(t,u)$ satisfies the Lipschitz condition with a Lipschitz constant $P>0$, given by:

$$|F_t(t,u_2) - F_t(t,u_1)| \leq P|u_2-u_1|,$$

then the FDE (2) possess a unique solution.

3 Proposed Scheme

In this proposed study, our primary focus is on numerically solving the IVP of FDEs given by:

$${}^{C}\mathscr{D}^{\rho}_{a^+} u = F(t,u), \;\; \text{with } u(a)=u_0, \text{ and } t \in [a, t_{end}]. \tag{3}$$

To proceed with our numerical approach, we utilize Lemma 2 to perform an analogous transformation. This results in obtaining the fractional order Caputo derivative of order $(1-\rho)$:

$$u' = {}^{C}\mathscr{D}^{1-\rho}_{a^+} F(t,u), \text{ with } u(a)=u_0, \text{ and } t \in [a, t_{end}]. \tag{4}$$

To achieve an accurate numerical technique for solving the corresponding (3), we are interested in finding the numerical solution of the IVP of FDEs (4). For this purpose, we have designed two numerical methods: Ralston's method (RM) and Ralston's method with two stages and minimum local error bound (RME). These methods have demonstrated higher accuracy and faster convergence compared to the existing methods EM and IEM.

3.1 Ralston Method of FDE

To obtain the approximate solution of (4) over the interval $J=[a,b]$, we propose an algorithm known as the Ralston method [31], which is a type of Runge-Kutta second-order scheme. The algorithm utilizes a set of equally spaced points (t_k,u_k) within the interval J, where the step length is denoted as $h=t_{k+1}-t_k$ for $k=0$ to N. The Ralston method scheme is as follows:

$$\begin{cases} t_k = t_0 + kh \;\; \text{for each} \;\; k=0 \text{ to } N, \\ \text{step length, } h = t_{k+1}-t_k, \\ u_{k+1} = u_k + \frac{h}{3}(l_1+2l_2), \text{ where} \\ l_1 = {}^{C}\mathscr{D}^{1-\rho}_{a^+} F(t,u_k)\big|_{t=t_k}, \\ l_2 = {}^{C}\mathscr{D}^{1-\rho}_{a^+} F(t+\frac{3h}{4}, u_k+\frac{3h}{4}l_1)\big|_{t=t_k}. \end{cases}$$

We use Matlab to demonstrate the efficiency and accuracy of the Ralston method algorithm. Before proceeding with the convergence results of our proposed method, we will present a few relevant lemmas that will be instrumental in proving the convergence.

Lemma 3. [28] If the function $F_t(t,u)$ satisfies the Lipschitz condition with a Lipschitz constant $P>0$, given by:

$$|F_t(t,u_2)-F_t(t,u_1)|\le P|u_2-u_1|,$$

and also meets the conditions stated in Theorem 1, then the function $\mathcal{G}(t,u)={}^{C}\mathscr{D}_{a^+}^{1-\rho}F(t,u)$ also holds the Lipschitz condition with another Lipschitz constant $M>0$,

$$|\mathcal{G}(t,u_2)-\mathcal{G}(t,u_1)|\le M|u_2-u_1|.$$

Lemma 4. If the function $\mathcal{G}(t,u)$ satisfies the Lipschitz condition with respect to the variable u and also meets the conditions stated in Theorem 1, then the expression

$$\Theta=\frac{1}{3}\mathcal{G}(t,u)+\frac{2}{3}\mathcal{G}\left(t+\frac{3h}{4},u+\frac{3h}{4}\mathcal{G}(t,u)\right)$$

also satisfies the Lipschitz condition.

Proof.

$$\begin{aligned}|\Theta(t,u_2)-\Theta(t,u_1)|&\le\frac{1}{3}|\mathcal{G}(t,u_2)-\mathcal{G}(t,u_1)|+\frac{2}{3}\left|\mathcal{G}\left(t+\frac{3h}{4},u_2+\frac{3h}{4}\mathcal{G}(t,u_2)\right)\right.\\&\qquad\left.-\mathcal{G}\left(t+\frac{3h}{4},u_1+\frac{3h}{4}\mathcal{G}(t,u_1)\right)\right|\\&\le\frac{M}{3}|u_2-u_1|+\frac{2M}{3}|u_2-u_1|+\frac{hM^2}{2}|u_2-u_1|\\&=M\left(1+\frac{hM}{2}\right)|u_2-u_1|\\&=P_\Theta|u_2-u_1|,\end{aligned}$$

So, $|\Theta(t,u_2)-\Theta(t,u_1)|\le P_\Theta|u_2-u_1|$, where $P_\Theta=M(1+\frac{hM}{2})$.

Theorem 3. Consider the function $F_t(t,u)$, which satisfies the Lipschitz condition with a Lipschitz constant $P>0$:

$$|F_t(t,u_2)-F_t(t,u_1)|\le P|u_2-u_1|.$$

Let $u(t)$ be the unique solution of (4). Suppose we use Ralston's method to generate the approximation u_k for each non-negative integer k from 0 to N. Then for each k,

$$u(t_k)-u_k=O(h^2).$$

Proof. Let the Ralston iterative scheme is based on $u_k=u(t_k)$, we have

$$\begin{aligned}\bar{u}_{k+1}=u(t_k)+\frac{h}{3}\Bigg[&{}^{C}\mathscr{D}_{a^+}^{1-\rho}F(t,u_k)\Big|_{t=t_k}\\&+2\,{}^{C}\mathscr{D}_{a^+}^{1-\rho}F\left(t+\frac{3h}{4},u_k+\frac{3h}{4}\,{}^{C}\mathscr{D}_{a^+}^{1-\rho}F(t,u_k)\Big|_{t=t_k}\right)\Bigg|_{t=t_k}\Bigg].\end{aligned}$$

Let us assume, $\mathcal{G}(t,u)={}^{C}\mathscr{D}_{a^+}^{1-\rho}F(t,u)$, then

$$\begin{aligned}\bar{u}_{k+1}&=u(t_k)+\frac{h}{3}\left[\mathcal{G}(t_k,u_k)+2\mathcal{G}\left(t_k+\frac{3h}{4},u_k+\frac{3h}{4}u'(t_k)\right)\right]\\&=u(t_k)+\frac{h}{3}\mathcal{G}(t_k,u_k)+\frac{2h}{3}\left[\mathcal{G}(t_k,u_k)+\frac{3h}{4}\left(\mathcal{G}_t(t_k,u_k)+\mathcal{G}_u(t_k,u_k)u'(t_k)\right)+\right.\\&\qquad\left.\frac{1}{2!}\left(\frac{3h}{4}\right)^2\left(\mathcal{G}_{tt}(\xi,\eta)+2u'(t_k)\,\mathcal{G}_{tu}(\xi,\eta)+(u'(t_k))^2\,\mathcal{G}_{uu}(\xi,\eta)\right)\right],\\&=u(t_k)+hu'(t_k)+\frac{h^2}{2}u''(t_k)+\frac{3h^3}{16}\left[\mathcal{G}_{tt}(\xi,\eta)+2u'(t_k)\mathcal{G}_{tu}(\xi,\eta)+(u'(t_k))^2\,\mathcal{G}_{uu}(\xi,\eta)\right].\end{aligned}\tag{5}$$

The exact form of the solution with the use of Taylor's series:

$$u(t_{k+1}) = u(t_k) + hu'(t_k) + \frac{h^2}{2!}u''(t_k) + \frac{h^3}{3!}u'''(t_k) + \dots \tag{6}$$

Using the expression (5) and (6), we get $u(t_{k+1}) - \bar{u}_{k+1} = O(h^3)$.

$$\text{So,} \quad |u(t_{k+1}) - \bar{u}_{k+1}| \le ch^3.$$

Let us assume that, $\Theta = \frac{1}{3}\mathcal{G}(t,u) + \frac{2}{3}\mathcal{G}\left(t + \frac{3h}{4}, u + \frac{3h}{4}\mathcal{G}(t,u)\right)$, then using the stated lemma (3) and (4), we have

$$\begin{aligned} |\bar{u}_{k+1} - u_{k+1}| &\le |u(t_k) - u_k| + h|\Theta(t_k, u(t_k)) - \Theta(t_k, u_k)|, \\ &\le (1 + hP_\Theta)|u(t_k) - u_k|. \end{aligned}$$

$$\begin{aligned} \text{Now,} \quad |u(t_{k+1}) - u_{k+1}| &\le |u(t_{k+1}) - \bar{u}_{k+1}| + |\bar{u}_{k+1} - u_{k+1}| \\ &\le ch^3 + (1 + hP_\Theta)|u(t_k) - u_k|. \end{aligned}$$

So we get the estimation, $|\epsilon_{k+1}| = (1 + hP_\Theta)|\epsilon_k| + ch^3$. Thus, we get,

$$|\epsilon_k| \le (1 + hP_\Theta)^k |e_0| + \frac{ch^2}{P_\Theta}\left[(1 + hP_\Theta)^k - 1\right].$$

As, $t_k - t_0 = hk$, and $\epsilon_0 = 0$ then, $(1 + hP_\Theta)^k \le e^{khP_\Theta} = \psi_\Theta$.
So we have, $|\epsilon_k| \le \frac{ch^2}{P_\Theta}(\psi_\Theta - 1)$.
Hence, $u(t_k) - u_k = O(h^2)$.
This signifies that order of convergence of Ralston's method is quadratic.

3.2 Ralston Method with Minimum Local Error Bound of FDE

This is also a second order Runge-Kutta method which is proposed by Anthony Ralston[32] where the local error bound of this scheme is minimum compare to other RK2 methods. According to RME, we obtain the following scheme for the IVP of FDEs (4):

$$\begin{cases} t_k = t_0 + kh \ \text{ for each } \ k = 0 \text{ to } N, \\ \text{step length, } h = t_{k+1} - t_k, \\ u_{k+1} = u_k + \frac{h}{4}(l_1 + 3l_2), \ \text{ where} \\ l_1 = {}^{C}\mathscr{D}_{a^+}^{1-\rho} F(t,u_k)\big|_{t=t_k}, \\ l_2 = {}^{C}\mathscr{D}_{a^+}^{1-\rho} F(t + \frac{2h}{3}, u_k + \frac{2h}{3}l_1)\big|_{t=t_k}. \end{cases}$$

This scheme improves the accuracy and the algorithm is more appropriate and accurate. In addition of this, this algorithm is better than the other numerical scheme of second order convergence for IVP (4) scheme and also in this scheme the amount of computation is very less to obtain the accurate result.

Lemma 5. If the function $\mathcal{G}(t,u)$ satisfies the Lipschitz condition with respect to the variable u and also meets the conditions stated in Theorem 1, then the expression

$$\Theta = \frac{1}{4}\,\mathcal{G}(t,u) + \frac{3}{4}\,\mathcal{G}\left(t + \frac{2h}{3}, u + \frac{2h}{3}\mathcal{G}(t,u)\right)$$

also satisfies the Lipschitz condition.

Proof:

$$\begin{aligned}|\Theta(t,u_2)-\Theta(t,u_1)| &\le \frac{1}{4}|\mathcal{G}(t,u_2)-\mathcal{G}(t,u_1)|+\frac{3}{4}\left|\mathcal{G}\left(t+\frac{2h}{3},u_2+\frac{2h}{3}\mathcal{G}(t,u_2)\right)\right.\\ &\qquad\left.-\mathcal{G}\left(t+\frac{2h}{3},u_1+\frac{2h}{3}\mathcal{G}(t,u_1)\right)\right|\\ &\le \frac{M}{4}|u_2-u_1|+\frac{3M}{4}|u_2-u_1|+\frac{hM^2}{2}|u_2-u_1|\\ &= M\left(1+\frac{hM}{2}\right)|u_2-u_1|\\ &= P_\Theta|u_2-u_1|,\end{aligned}$$

So, $|\Theta(t,u_2)-\Theta(t,u_1)| \le P_\Theta|u_2-u_1|$, where $P_\Theta = M(1+\frac{hM}{2})$.

Theorem 4. Consider the function $F_t(t,u)$, which satisfies the Lipschitz condition with respect to the variable u and a Lipschitz constant $P>0$:

$$|F_t(t,u_2)-F_t(t,u_1)| \le P|u_2-u_1|,$$

Let $u(t)$ posses the unique solution of (4). Suppose we use Ralston's method to generate the approximation u_k with minimum local error bound for each non-negative integer k from 0 to N. Then, for each k,

$$u(t_k)-u_k = O(h^2).$$

Proof. Based on the assumption that the Ralston iterative scheme has a minimum local error bound, and considering u_k as $u(t_k)$, then we have

$$\begin{aligned}\bar{u}_{k+1} = u(t_k)+\frac{h}{4}\Bigg[&{}^{C}\mathscr{D}_{a^+}^{1-\rho}F(t,u_k)\Big|_{t=t_k}\\ &+3\,{}^{C}\mathscr{D}_{a^+}^{1-\rho}F\left(t+\frac{2h}{3},u_k+\frac{2h}{3}\,{}^{C}\mathscr{D}_{a^+}^{1-\rho}F(t,u_k)\Big|_{t=t_k}\right)\Bigg|_{t=t_k}\Bigg].\end{aligned}$$

Let us assume, $\mathcal{G}(t,u) = {}^{C}\mathscr{D}_{a^+}^{1-\rho}F(t,u)$, then

$$\begin{aligned}\bar{u}_{k+1} &= u(t_k)+\frac{h}{4}\left[\mathcal{G}(t_k,u_k)+3\mathcal{G}\left(t_k+\frac{2h}{3},u_k+\frac{2h}{3}u'(t_k)\right)\right]\\ &= u(t_k)+\frac{h}{4}\mathcal{G}(t_k,u_k)+\frac{3h}{4}\left[\mathcal{G}(t_k,u_k)+\frac{2h}{3}\left(\mathcal{G}_t(t_k,u_k)+\mathcal{G}_u(t_k,u_k)u'(t_n)\right)+\right.\\ &\qquad\left.\frac{1}{2!}\left(\frac{2h}{3}\right)^2\left(\mathcal{G}_{tt}(\xi,\eta)+2u'(t_k)\,\mathcal{G}_{tu}(\xi,\eta)+(u'(t_k))^2\mathcal{G}_{uu}(\xi,\eta)\right)\right]\\ &= u(t_k)+hu'(t_k)+\frac{h^2}{2}u''(t_k)+\frac{h^3}{6}\left[\mathcal{G}_{tt}(\xi,\eta)+2u'(t_k)\mathcal{G}_{tu}(\xi,\eta)+(u'(t_k))^2\mathcal{G}_{uu}(\xi,\eta)\right]\end{aligned} \tag{7}$$

The exact form of the solution with the use of Taylor series:

$$u(t_{k+1}) = u(t_k)+hu'(t_k)+\frac{h^2}{2!}u''(t_k)+\frac{h^3}{3!}u'''(t_k)+\ldots \tag{8}$$

Using the expression (7) and (8), we get $u(t_{k+1})-\bar{u}_{k+1} = O(h^3)$.

$$\text{So,}\quad |u(t_{k+1})-\bar{u}_{k+1}| \le ch^3.$$

Let us assume that, $\Theta = \frac{1}{4}\mathcal{G}(t,u)+\frac{3}{4}\mathcal{G}\left(t+\frac{2h}{3},u+\frac{2h}{3}\mathcal{G}(t,u)\right)$, then using the stated lemma (3) and (5), we have

$$\begin{aligned}|\bar{u}_{k+1}-u_{k+1}| &\le |u(t_k)-u_k|+h|\Theta(t_k,u(t_k))-\Theta(t_k,u_k)|\\ &\le (1+hP_\Theta)|u(t_k)-u_k|.\end{aligned}$$

$$\text{Now, } |u(t_{k+1}) - u_{k+1}| \le |u(t_{k+1}) - \bar{u}_{k+1}| + |\bar{u}_{k+1} - u_{k+1}|$$
$$\le ch^3 + (1 + hP_\Theta)|u(t_k) - u_k|.$$

So, we get the estimation, $|\epsilon_{k+1}| = (1 + hP_\Theta)|\epsilon_k| + ch^3$.
Thus,

$$|\epsilon_k| \le (1 + hP_\Theta)^k |e_0| + \frac{ch^2}{P_\Theta}\Big[(1 + hP_\Theta)^k - 1\Big].$$

As, $t_k - t_0 = hk$, and $\epsilon_0 = 0$ then, $(1 + hP_\Theta)^k \le e^{khP_\Theta} = \psi_\Theta$.
So we have, $|\epsilon_k| \le \frac{ch^2}{P_\Theta}(\psi_\Theta - 1)$.
Hence, $u(t_k) - u_k = O(h^2)$.
This signifies that order of convergence of the Ralston's method with minimum local error bound is quadratic.

4 Numerical Discussion

In this part of section, we have considered four numerical examples IVP of FDEs and which are numerically investigated with our proposed technique using Matlab. In such four problem, the first IVP of FDE is our world population growth model and after that the next two IVP of FDEs are based on linear FDEs ant at the last one example is based on non-linear FDE. Basically, we illustrate the numerical stability, convergence and order of EM, IEM, and our suggested algorithmic RM and RME by the comparison of the exact and numerical solution of FDEs in both tabular and graphical form.

Example 1(Population Growth Model). Consider the IVP of a FDE for the population growth model as given in [48]:,

$$^{C}\mathscr{D}^{\rho}_{0^+}\mathbb{N}(t) = P\mathbb{N}(t), \quad t \ge 0, \tag{9}$$
$$\mathbb{N}(0) = \mathbb{N}_0.$$

Here, the individuals population is denoted by $\mathbb{N}(t)$ at given time t, while $P = B - M$ indicating the production rate in which M is the mortality rate, and B is the birth rate. When $\rho = 1$, the model simplifies to the classical linear population growth model. The classical model of population growth described by (9) has an exact solution given by: $\mathbb{N}(t) = \mathbb{N}_0 \exp(Pt)$, $t \ge 0$.

However, in our fractional model, we observe that the statistical population data collected from various sources matches well with our model for $\rho = 1.39329875484$. The fractional model of population growth described by (9) has an exact solution given by: $\mathbb{N}(t) = \mathbb{N}_0\, E_\rho(Pt)$, $t \ge 0$, where E_ρ is the Mittag-Leffler function.

By applying our proposed numerical methodology, we obtain the numerical results for (9) with different values of ρ and step length $h = 1$. The results are graphically illustrated in Figure 1 and Figure 2, and tabulated in Table 1 and 2. Additionally, the absolute error is shown in Figure 3. It can be clearly seen that our suggested methods RM and RME outperform EM and IEM in terms of accuracy.

Table 1: Numerical result of Example 1 for $\rho = 1,\ 1.39329875484$, and $h = 1$.

	Exact		EM		IEM		RM	
Year	$\mathbb{N}_{linear}$	$\mathbb{N}_{frac}$	$\mathbb{N}_{EM}$	$\lvert\mathbb{N}_{EM} - \mathbb{N}_{frac}\rvert$	$\mathbb{N}_{IEM}$	$\lvert\mathbb{N}_{IEM} - \mathbb{N}_{frac}\rvert$	$\mathbb{N}_{RM}$	$\lvert\mathbb{N}_{RM} - \mathbb{N}_{frac}\rvert$
1920	1860.0000	1860.0000	1860.0000	0.0000	1860.0000	0.0000	1860.0000	0.0000
1930	2128.8597	1990.9106	1979.8511	11.0596	1989.1791	1.7315	1989.9802	0.9304
1940	2436.5826	2216.9054	2201.9843	14.9211	2215.1641	1.7413	2215.9724	0.9330
1950	2788.7863	2517.3204	2498.6957	18.6247	2515.5814	1.7390	2516.3880	0.9324
1960	3191.9004	2894.3102	2871.6952	22.6150	2892.5781	1.7320	2893.3795	0.9307
1970	3653.2840	3356.0765	3328.9598	27.1167	3354.3545	1.7219	3355.1482	0.9282
1980	4181.3597	3914.7154	3882.4076	32.3078	3913.0065	1.7090	3913.7904	0.9250
1990	4785.7679	4585.8060	4547.4431	38.3629	4584.1130	1.6930	4584.8850	0.9210
2000	5477.5422	5388.5478	5343.0767	45.4711	5386.8741	1.6737	5387.6315	0.9162
2010	6269.3112	6346.1698	6292.3229	53.8468	6344.5192	1.6505	6345.2593	0.9105
2020	7175.5290	7486.5286	7422.7899	63.7388	7484.9057	1.6229	7485.6250	0.9036

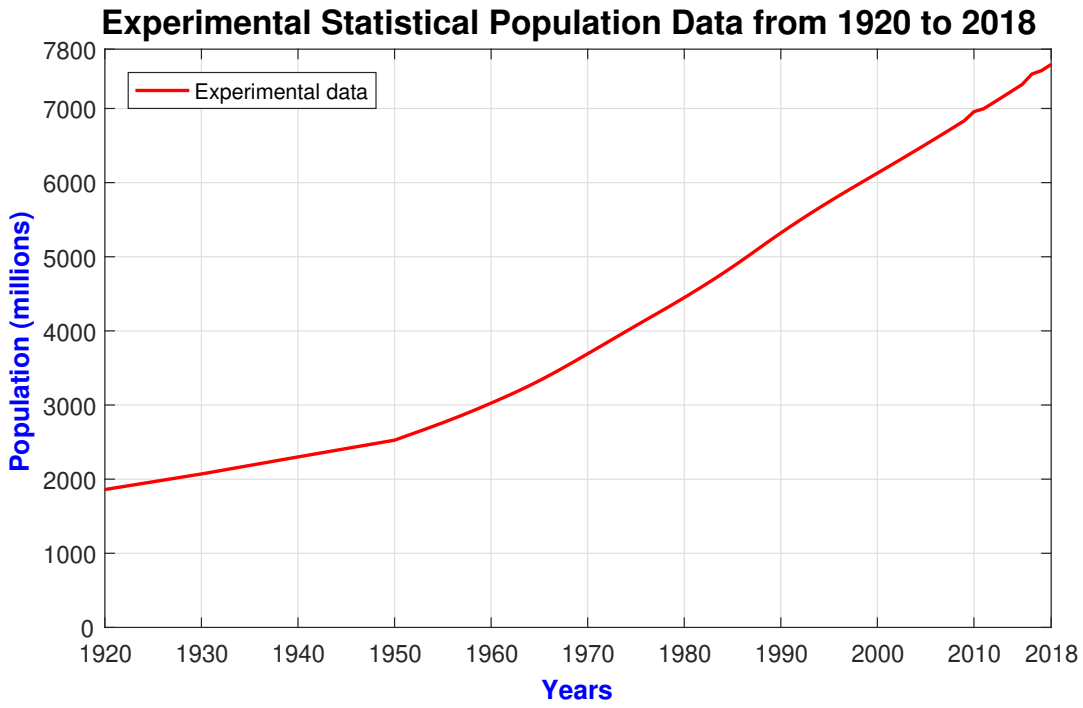

Fig. 1: World population data from 1920 to 2018

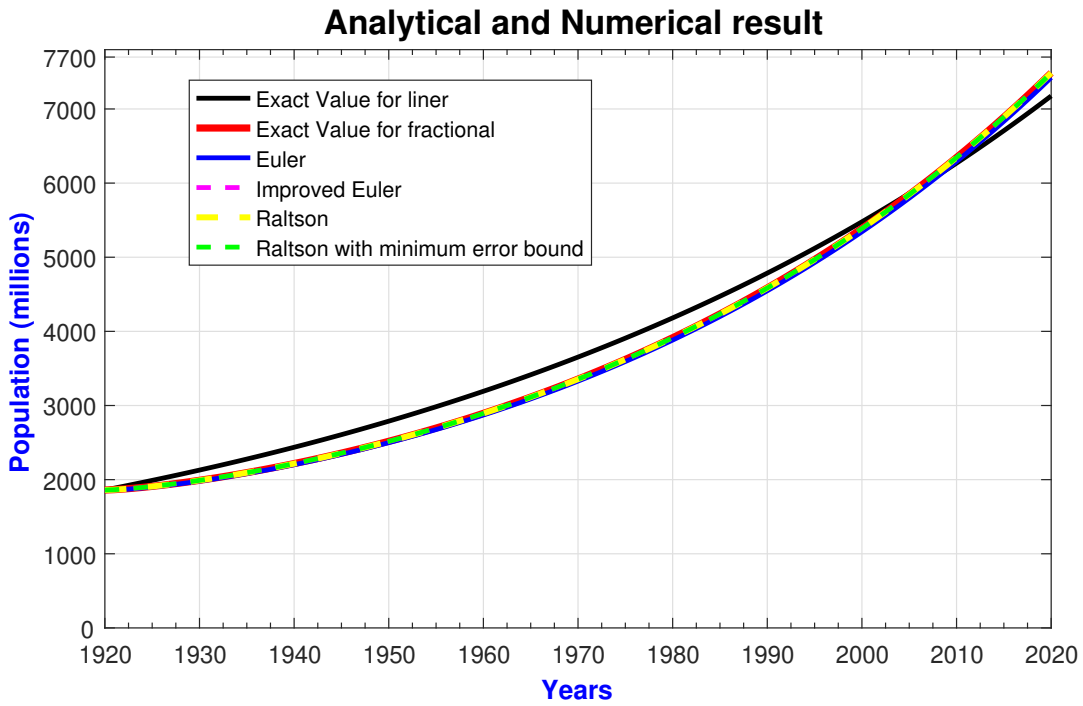

Fig. 2: Exact and numerical result of Example 1

Table 2: Numerical result of Example 1 for $\rho = 1,\ 1.39329875484$, and $h = 1$.

	Exact		EM		IEM		RME	
Year	$\mathbb{N}_{linear}$	$\mathbb{N}_{frac}$	$\mathbb{N}_{EM}$	$\lvert\mathbb{N}_{EM} - \mathbb{N}_{frac}\rvert$	$\mathbb{N}_{IEM}$	$\lvert\mathbb{N}_{IEM} - \mathbb{N}_{frac}\rvert$	$\mathbb{N}_{RME}$	$\lvert\mathbb{N}_{RME} - \mathbb{N}_{frac}\rvert$
1920	1860.0000	1860.0000	1860.0000	0.0000	1860.0000	0.0000	1860.0000	0.0000
1930	2128.8597	1990.9106	1979.8511	11.0596	1989.1791	1.7315	1990.3391	0.5715
1940	2436.5826	2216.9054	2201.9843	14.9211	2215.1641	1.7413	2216.3337	0.5717
1950	2788.7863	2517.3204	2498.6957	18.6247	2515.5814	1.7390	2516.7487	0.5717
1960	3191.9004	2894.3102	2871.6952	22.6150	2892.5781	1.7320	2893.7385	0.5717
1970	3653.2840	3356.0765	3328.9598	27.1167	3354.3545	1.7219	3355.5047	0.5717
1980	4181.3597	3914.7154	3882.4076	32.3078	3913.0065	1.7090	3914.1437	0.5718
1990	4785.7679	4585.8060	4547.4431	38.3629	4584.1130	1.6930	4585.2342	0.5718
2000	5477.5422	5388.5478	5343.0767	45.4711	5386.8741	1.6737	5387.9760	0.5718
2010	6269.3112	6346.1698	6292.3229	53.8468	6344.5192	1.6505	6345.5980	0.5718
2020	7175.5290	7486.5286	7422.7899	63.7388	7484.9057	1.6229	7485.9568	0.5718

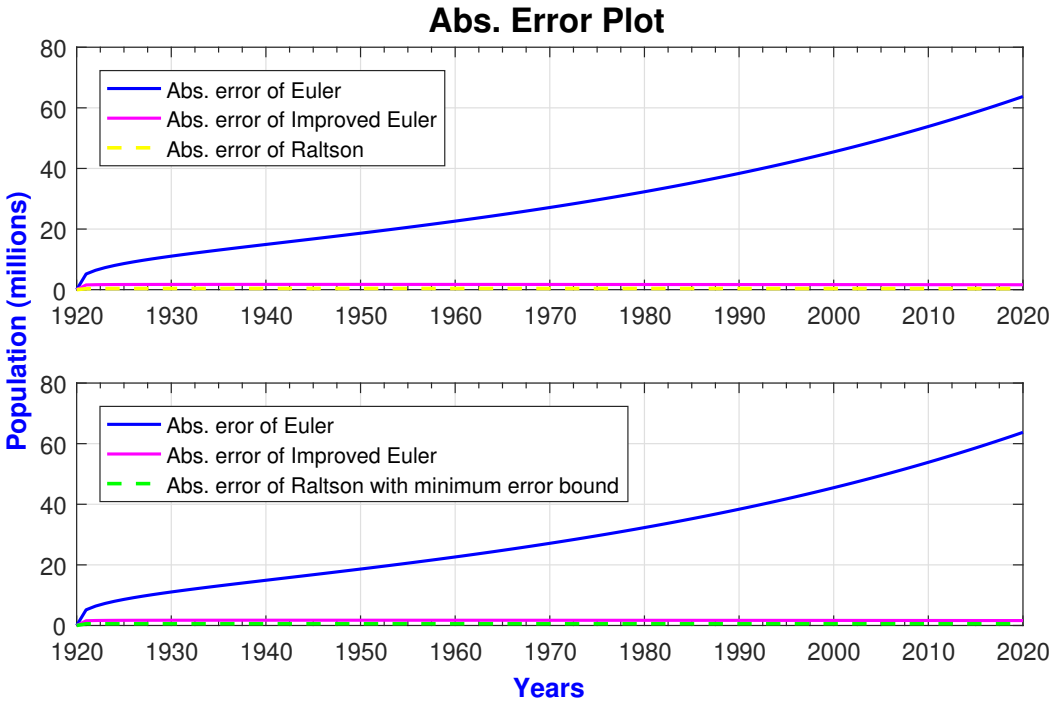

Fig. 3: Abs. error plot for Example 1

As of June 2018, The Census Bureau's International Data Base estimated the world population to be around 7500 million, which closely aligns with our fractional model's estimate when we assume $\rho = 1.39329875484$. The numerical results obtained through RM and RME demonstrate higher accuracy and efficiency compared to other numerical schemes like EM and IEM. This highlights the reliability and effectiveness of our proposed methodology in approximating the population growth model.

Example 2. Consider the below IVP of linear FDE,

$$\begin{aligned} {}^{C}\mathscr{D}^{\rho}_{0^+} u &= t^3,\ t \in [0,1], \\ u(0) &= 0. \end{aligned} \tag{10}$$

For $\rho = 0.5$, exact solution of (10) is,

$$u(t) = \frac{32}{35\sqrt{\pi}} t^{3.5}.$$

With the assistance of the suggested methodology using Matlab, we have obtained the numerical results for $\rho = 0.5$ with a step length of $h = 0.1$. The graphical representation of the numerical and exact solutions of (10) is presented in Figure 4, which shows a comparison between the suggested method, EM, and IEM. Tables 3 and 4 provide a detailed comparison of the exact values, approximate values, and absolute errors obtained using EM, IEM, RM, and RME methods. It is evident from the tables that the numerical solutions obtained from RM and RME are highly accurate and closely approximate the exact solution of the problem. Figure 5 displays the absolute errors of EM, IEM, RM, and RME. It is evident that RM and RME exhibit the minimum absolute error compared to EM and IEM, while IEM, RM, and RME have the same order of convergence. Additionally, RME performs better than RM since RME incorporates a minimum local error bound.

The estimated order of convergence (EOC) for EM, IEM, RM, and RME is summarized in Table 5 and depicted graphically in Figure 6. The figure illustrates the linear convergence of EM (blue color) and the quadratic convergence of IEM (magenta color), RM (red color), and RME (green color). Overall, the results demonstrate that our suggested methods RM and RME offer quadratic convergence and are more accurate than EM and IEM. From the results obtained in Example 2, we can conclude that both RM and RME are significantly more accurate compared to EM and IEM. Among the two methods, RME exhibits even higher accuracy as it incorporates a minimum local error bound, surpassing all other second-order convergence methods.

Similar conclusions can be drawn from the results of Example 3 and Example 4, where RM and RME once again outperform EM and IEM in terms of accuracy and efficiency. RME consistently demonstrates superior accuracy due to its minimum local error bound.

Table 3: Numerical result of Example 2 for $\rho = 0.5$ and $h = 0.1$.

		EM		IEM		RM	
x	u	u_{EM}	$\lvert u-u_{EM}\rvert$	u_{IEM}	$\lvert u-u_{IEM}\rvert$	u_{RM}	$\lvert u-u_{RM}\rvert$
.00	.00000	.00000	.00000000	.00000	.00000000	.00000	.00000000
.10	.00016	.00000	.00016312	.00029	.00012234	.00019	.00002229
.20	.00185	.00057	.00127457	.00219	.00034023	.00192	.00007221
.30	.00763	.00380	.00382783	.00825	.00062204	.00777	.00013914
.40	.02088	.01270	.00817906	.02184	.00095565	.02110	.00021956
.50	.04559	.03097	.01462369	.04693	.00133401	.04590	.00031152
.60	.08631	.06289	.02341998	.08806	.00175233	.08672	.00041373
.70	.14803	.11323	.03480040	.15024	.00220713	.14856	.00052524
.80	.23622	.18724	.04897808	.23892	.00269568	.23687	.00064535
.90	.35674	.29059	.06615096	.35996	.00321579	.35752	.00077346
1.00	.51583	.42933	.08650468	.51960	.00376566	.51674	.00090912

Table 4: Numerical result of Example 2 for $\rho = 0.5$ and $h = 0.1$.

		EM		IEM		RME	
x	u	u_{EM}	$\lvert u-u_{EM}\rvert$	u_{IEM}	$\lvert u-u_{IEM}\rvert$	u_{RME}	$\lvert u-u_{RME}\rvert$
.00	.00000	.00000	.00000000	.00000	.00000000	.00000	.00000000
.10	.00016	.00000	.00016312	.00029	.00012234	.00016	.00000774
.20	.00185	.00057	.00127457	.00219	.00034023	.00183	.00001185
.30	.00763	.00380	.00382783	.00825	.00062204	.00761	.00001501
.40	.02088	.01270	.00817906	.02184	.00095565	.02086	.00001767
.50	.04559	.03097	.01462369	.04693	.00133401	.04557	.00002002
.60	.08631	.06289	.02341998	.08806	.00175233	.08628	.00002214
.70	.14803	.11323	.03480040	.15024	.00220713	.14801	.00002409
.80	.23622	.18724	.04897808	.23892	.00269568	.23620	.00002590
.90	.35674	.29059	.06615096	.35996	.00321579	.35672	.00002761
1.00	.51583	.42933	.08650468	.51960	.00376566	.51580	.00002922

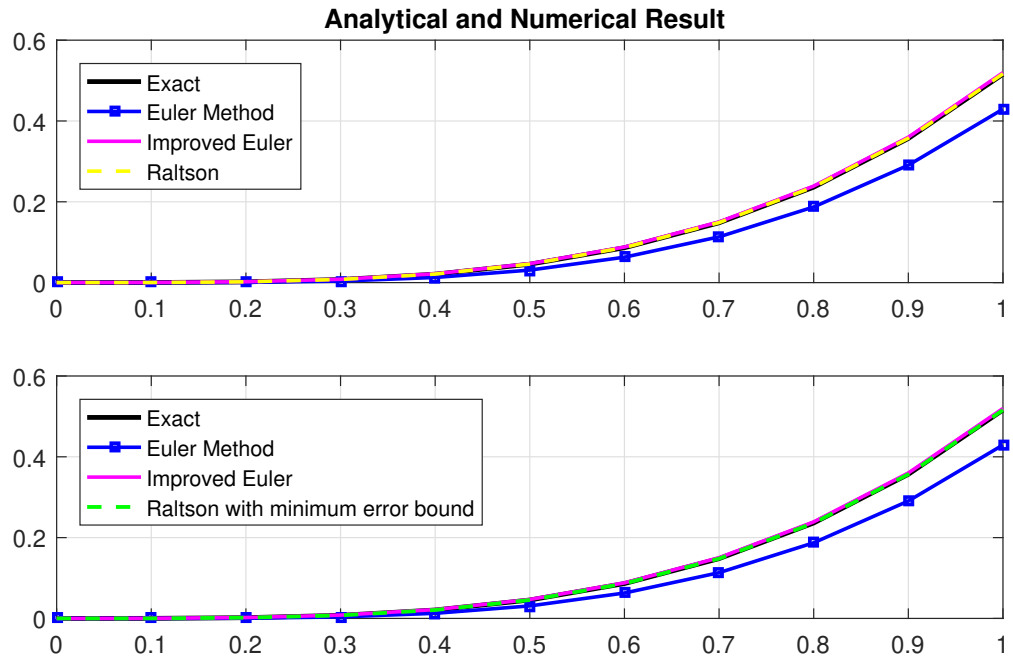

Fig. 4: Exact and numerical result of Example 2

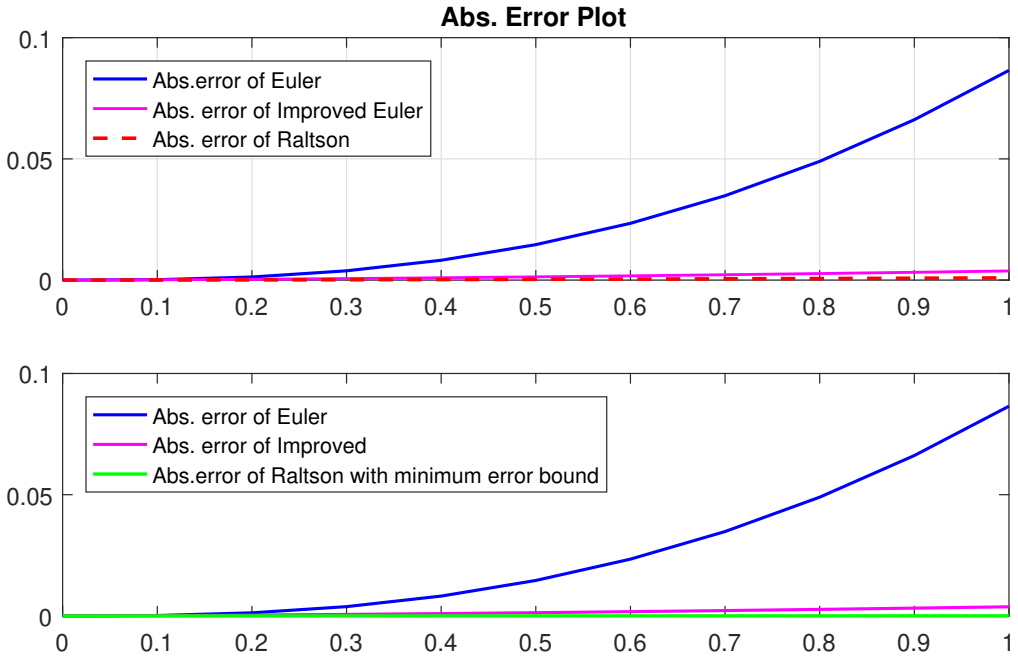

Fig. 5: Abs. error plot for Example 2

Table 5: Table of order for Example 2

	EM		IEM		RM		RME	
n	$\|u-u_{EM}\|$	EOC	$\|u-u_{IEM}\|$	EOC	$\|u-u_{RM}\|$	EOC	$\|u-u_{RME}\|$	EOC
10	.086505	—	.003766	—	.000909	—	.0018842235	—
20	.044194	.968913	.000941	2.001070	.000231	1.976364	.0004704861	2.00174617
40	.022332	.984723	.000235	2.000392	.000058	1.987750	.0001175692	2.00064236
80	.011225	.992425	.000059	2.000142	.000015	1.993707	.0000293875	2.00023330
160	.005627	.996228	.000015	2.000051	.000004	1.996790	.0000073465	2.00008403
320	.002817	.998118	.000004	2.000018	.000001	1.998371	.0000018366	2.00003009
640	.001410	.999060	.000001	2.000007	.000000	1.999177	.0000004591	2.00001073
1280	.000705	.999530	.000000	2.000002	.000000	1.999585	.0000001148	2.00000381

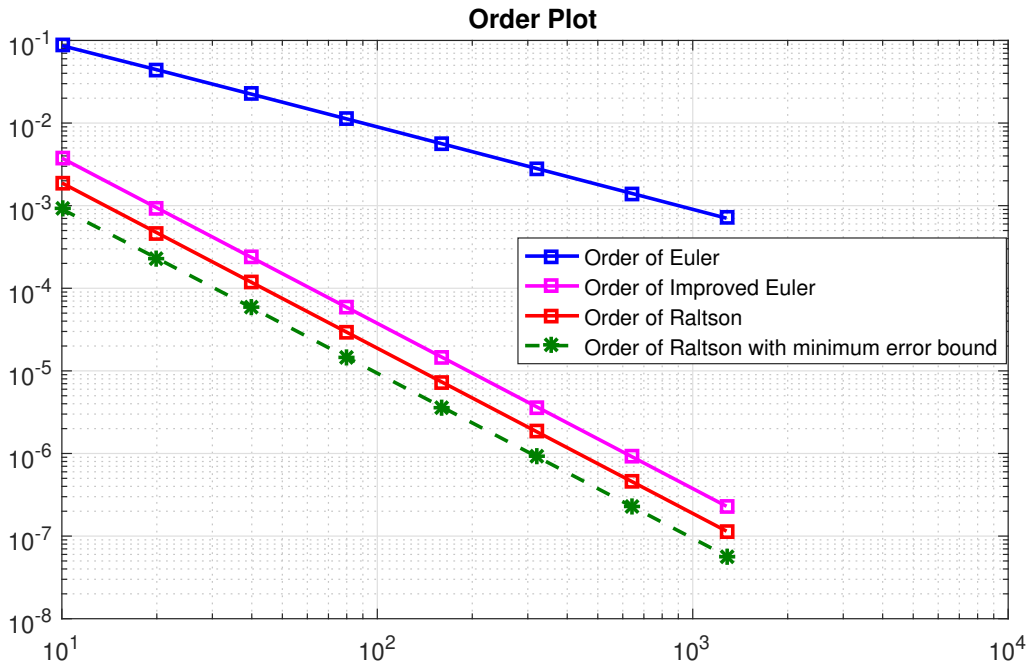

Fig. 6: Order graph of Example 2

Example 3. Let us consider the following IVP of linear FDE [49]:

$$\begin{aligned} {}^{C}\mathscr{D}^{\rho}_{0^+}u &= -u,\ t\in[0.1,1], \\ u(0.1) &= E_{\rho}(-(0.1)^{\rho}). \end{aligned} \tag{11}$$

For $\rho = 0.5$, exact solution of (11) is,

$$u(t) = E_{\rho}(-t^{\rho}).$$

The numerical results of (11) for $\rho = 0.5$ with a step length of $h = 0.1$ are graphically presented in Figure 7. The exact and approximate solutions are tabulated in Table 6 and Table 7 for comparison.

Moreover, the error plot in Figure 8 illustrates the absolute error of EM, IEM, RM, and RME. It is evident that RM and RME demonstrate smaller absolute errors compared to EM and IEM. Additionally, the EOC for each method is listed in Table 8. Figure 9 visually displays the convergence behavior of the numerical methods. The blue color indicates the convergence of EM which is linear, while the magenta, red, and green colors signify the quadratic convergence of IEM, RM, and RME, respectively. It is evident from the figure that EM has a linear, whereas IEM, RM, and RME exhibit a faster quadratic convergence rate.

Table 6: Numerical result of Example 3 for $\rho = 0.5$ and $h = 0.1$.

		EM		IEM		RM	
x	u	u_{EM}	$\lvert u-u_{EM}\rvert$	u_{IEM}	$\lvert u-u_{IEM}\rvert$	u_{RM}	$\lvert u-u_{RM}\rvert$
.10	.72358	.72358	.00000000	.72358	.00000000	.72358	.00000000
.20	.64379	.61752	.02626440	.63966	.00412602	.64232	.00146708
.30	.59202	.55575	.03627234	.58687	.00514736	.59023	.00178836
.40	.55361	.51194	.04166479	.54805	.00556030	.55170	.00191094
.50	.52316	.47810	.04506071	.51739	.00576982	.52119	.00197107
.60	.49802	.45062	.04740149	.49213	.00589126	.49602	.00200514
.70	.47670	.42759	.04911376	.47073	.00596811	.47468	.00202636
.80	.45825	.40783	.05042033	.45223	.00601990	.45621	.00204049
.90	.44202	.39057	.05144943	.43596	.00605647	.43997	.00205038
1.00	.42758	.37530	.05228025	.42150	.00608327	.42553	.00205757

Table 7: Numerical result of Example 3 for $\rho = 0.5$ and $h = 0.1$.

		EM		IEM		RME	
x	u	u_{EM}	$\lvert u-u_{EM}\rvert$	u_{IEM}	$\lvert u-u_{IEM}\rvert$	u_{RME}	$\lvert u-u_{RME}\rvert$
.10	.72358	.72358	.00000000	.72358	.00000000	.72358	.00000000
.20	.64379	.61752	.02626440	.63966	.00412602	.64336	.00042650
.30	.59202	.55575	.03627234	.58687	.00514736	.59153	.00048880
.40	.55361	.51194	.04166479	.54805	.00556030	.55310	.00050679
.50	.52316	.47810	.04506071	.51739	.00576982	.52264	.00051392
.60	.49802	.45062	.04740149	.49213	.00589126	.49751	.00051732
.70	.47670	.42759	.04911376	.47073	.00596811	.47618	.00051915
.80	.45825	.40783	.05042033	.45223	.00601990	.45773	.00052022
.90	.44202	.39057	.05144943	.43596	.00605647	.44150	.00052090
1.00	.42758	.37530	.05228025	.42150	.00608327	.42706	.00052134

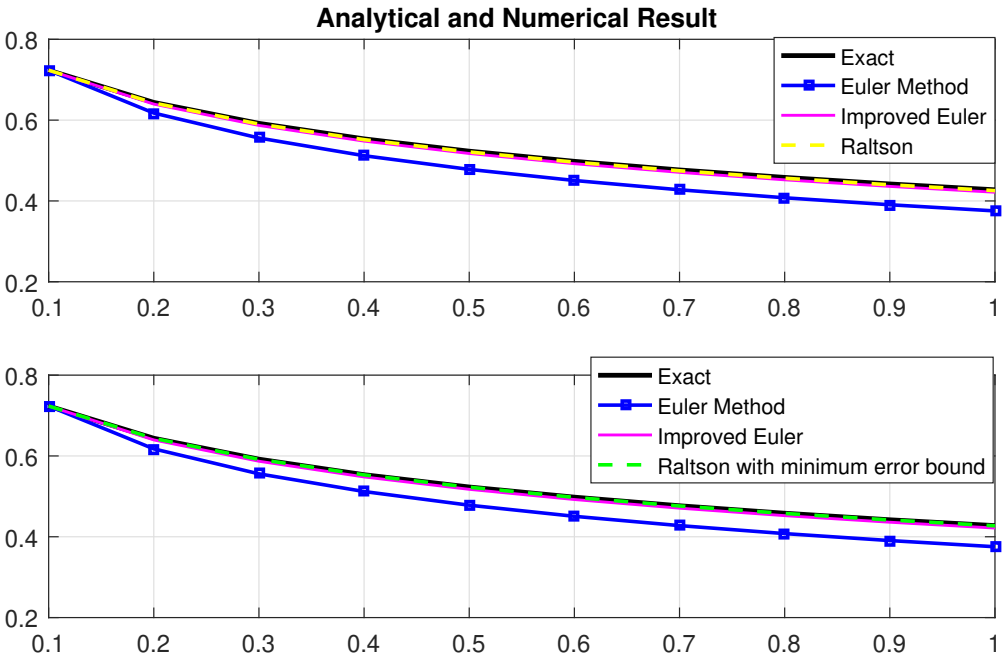

Fig. 7: Exact & approximate solution of Example 3

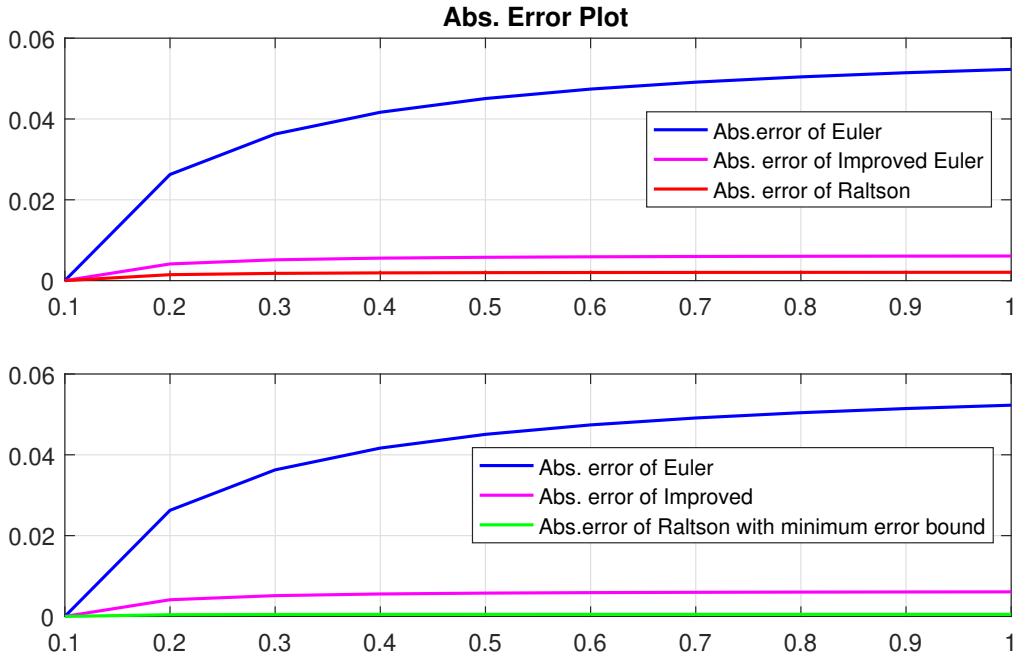

Fig. 8: Abs. error plot for Example 3

Table 8: Table of order for Example 3

	EM		IEM		RM		RME	
n	$\lvert u-u_{EM}\rvert$	EOC	$\lvert u-u_{IEM}\rvert$	EOC	$\lvert u-u_{RM}\rvert$	EOC	$\lvert u-u_{RME}\rvert$	EOC
15	.065838	—	.003230	—	.001596	—	.0009330781	—
30	.033717	.965436	.000817	1.983248	.000407	1.970917	.0002209644	2.07818372
60	.017062	.982680	.000205	1.995398	.000102	1.991965	.0000533592	2.05000516
120	.008582	.991370	.000051	1.998817	.000026	1.997931	.0000130857	2.02774084
240	.004304	.995698	.000013	1.999702	.000006	1.999479	.0000032387	2.01452211
480	.002155	.997853	.000003	1.999925	.000002	1.999869	.0000008055	2.00741740
960	.001078	.998928	.000001	1.999981	.000000	1.999967	.0000002009	2.00374679
1920	.000539	.999464	.000000	1.999995	.000000	1.999992	.0000000501	2.00188327

Example 4. Let us consider the following IVP of nonlinear FDE:

$$ {}^{C}\mathscr{D}^{\rho}_{1^+}u = \left(\frac{\Gamma(4.5)}{6}\right)^{\frac{6}{7}} u^{\frac{6}{7}},\ t\in[1,2], \tag{12} $$
$$ u(1) = \frac{6}{\Gamma(4.5)}. $$

For $\rho = 0.5$, exact solution of (12) is,

$$ u(t) = \frac{6}{\Gamma(4.5)} t^{\frac{7}{2}}. $$

The numerical results of (12) for $\rho = 0.5$ with a step length of $h = 0.1$ are depicted in Figure 10. The exact and approximate solutions are presented in Table 6 and Table 10 for comparison.

Additionally, the error plot in Figure 11 shows the absolute error of EM, IEM, RM, and RME. It is evident that RM and RME exhibit smaller absolute errors compared to EM and IEM. The EOC for each method is provided in Table 11. Figure 12 visually displays the convergence behavior of the numerical methods. The blue color indicates the convergence of EM which is linear, while the magenta, red, and green colors signify the quadratic convergence of IEM, RM, and RME,

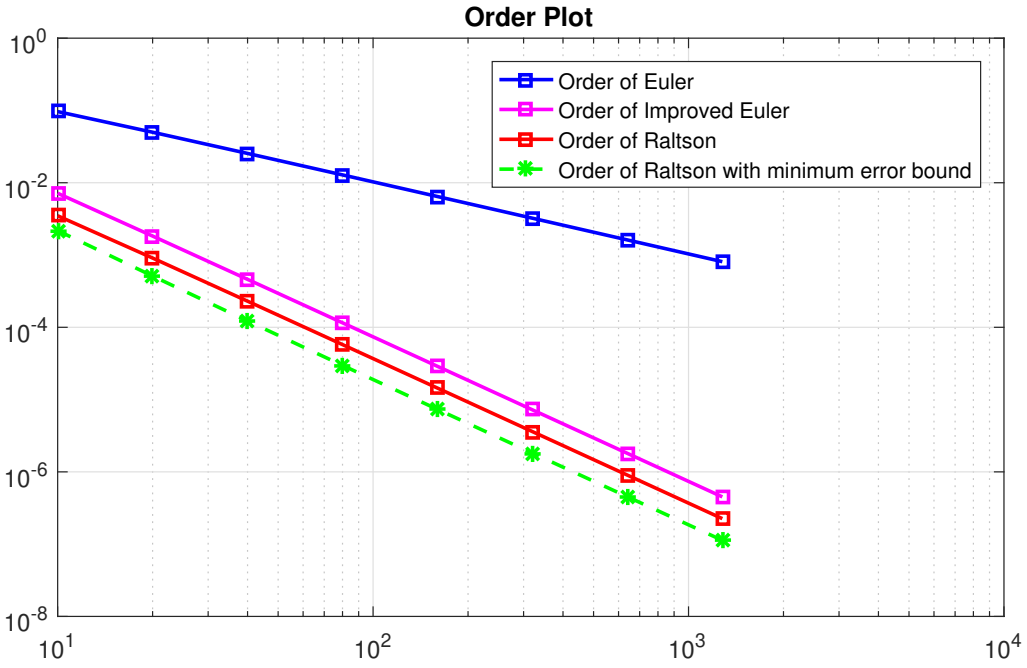

Fig. 9: Order graph of Example 3

respectively. It is evident from the figure that EM has a linear, whereas IEM, RM, and RME exhibit a faster quadratic convergence rate.

Table 9: Numerical result of Example 4 for $\rho = 0.5$ and $h = 0.1$.

		EM		IEM		RM	
x	u	u_{EM}	$\lvert u-u_{EM}\rvert$	u_{IEM}	$\lvert u-u_{IEM}\rvert$	u_{RM}	$\lvert u-u_{RM}\rvert$
1.00	.51583	.51583	.00000000	.51583	.00000000	.51583	.00000000
1.10	.72008	.69637	.02370993	.71795	.00212908	.71818	.00190563
1.20	.97643	.92007	.05635703	.97154	.00488883	.97206	.00437240
1.30	1.29214	1.19303	.09911207	1.28381	.00832293	1.28470	.00743877
1.40	1.67477	1.52163	.15313726	1.66230	.01247259	1.66363	.01114106
1.50	2.13219	1.91261	.21958539	2.11482	.01737686	2.11668	.01551372
1.60	2.67256	2.37296	.29959937	2.64948	.02307300	2.65197	.02058958
1.70	3.30429	2.90998	.39431192	3.27469	.02959667	3.27789	.02640011
1.80	4.03609	3.53124	.50484549	3.99911	.03698208	4.00311	.03297551
1.90	4.87691	4.24460	.63231224	4.83165	.04526220	4.83656	.04034487
2.00	5.83596	5.05814	.77781415	5.78149	.05446886	5.78742	.04853629

Table 10: Numerical result of Example 4 when $\rho = 0.5$ and $h = 0.1$.

		EM		IEM		RME	
x	u	u_{EM}	$\lvert u-u_{EM}\rvert$	u_{IEM}	$\lvert u-u_{IEM}\rvert$	u_{RME}	$\lvert u-u_{RME}\rvert$
1.00	.51583	.51583	.00000000	.51583	.00000000	.51583	.00000000
1.10	.72008	.69637	.02370993	.71795	.00212908	.71825	.00182808
1.20	.97643	.92007	.05635703	.97154	.00488883	.97224	.00419342
1.30	1.29214	1.19303	.09911207	1.28381	.00832293	1.28500	.00713272
1.40	1.67477	1.52163	.15313726	1.66230	.01247259	1.66409	.01068063
1.50	2.13219	1.91261	.21958539	2.11482	.01737686	2.11732	.01487005
1.60	2.67256	2.37296	.29959937	2.64948	.02307300	2.65282	.01973234
1.70	3.30429	2.90998	.39431192	3.27469	.02959667	3.27899	.02529752
1.80	4.03609	3.53124	.50484549	3.99911	.03698208	4.00449	.03159445
1.90	4.87691	4.24460	.63231224	4.83165	.04526220	4.83826	.03865090
2.00	5.83596	5.05814	.77781415	5.78149	.05446886	5.78946	.04649372

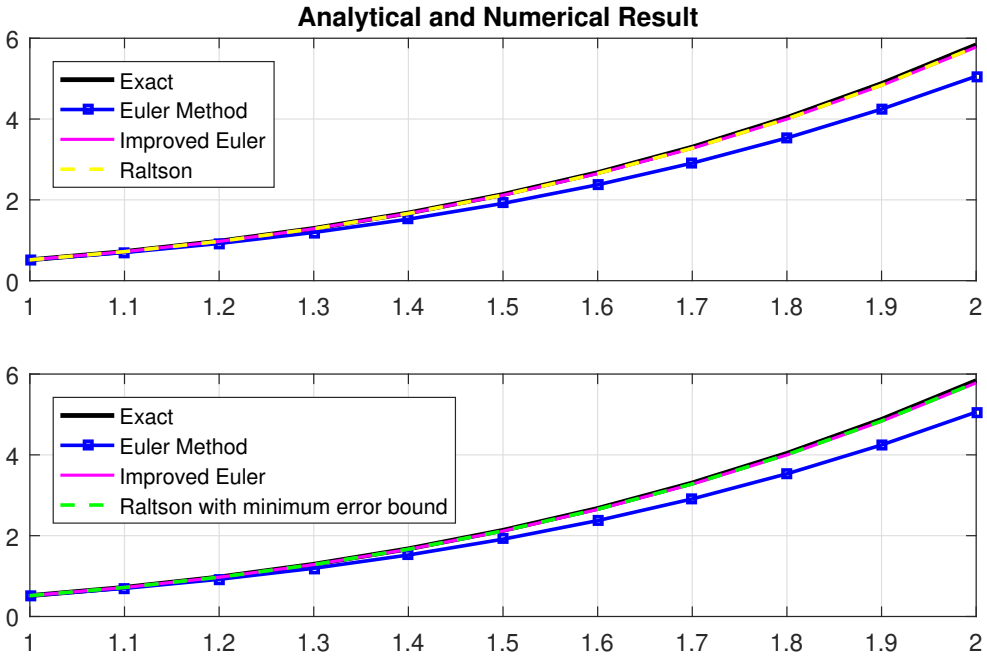

Fig. 10: Analytical & approximate solution of Example 4

Table 11: Table of order for Example 4

	EM		IEM		RM		RME	
n	$\lvert u-u_{EM}\rvert$	EOC	$\lvert u-u_{IEM}\rvert$	EOC	$\lvert u-u_{RM}\rvert$	EOC	$\lvert u-u_{RME}\rvert$	EOC
10	.777814	—	.054469	—	.048536	—	.046493724	—
20	.414226	.909007	.014722	1.887456	.013007	1.899750	.012425634	1.9037164
40	.213974	.952986	.003831	1.942365	.003369	1.949119	.003213153	1.9512578
80	.108774	.976105	.000977	1.970811	.000857	1.974362	.000817060	1.9754746
160	.054843	.987954	.000247	1.985308	.000216	1.987130	.000206014	1.9876980
320	.027537	.993952	.000062	1.992629	.000054	1.993552	.000051724	1.9938391
640	.013797	.996970	.000016	1.996308	.000014	1.996773	.000012958	1.9969170
1280	.006906	.998483	.000004	1.998152	.000003	1.998386	.000003243	1.9984579

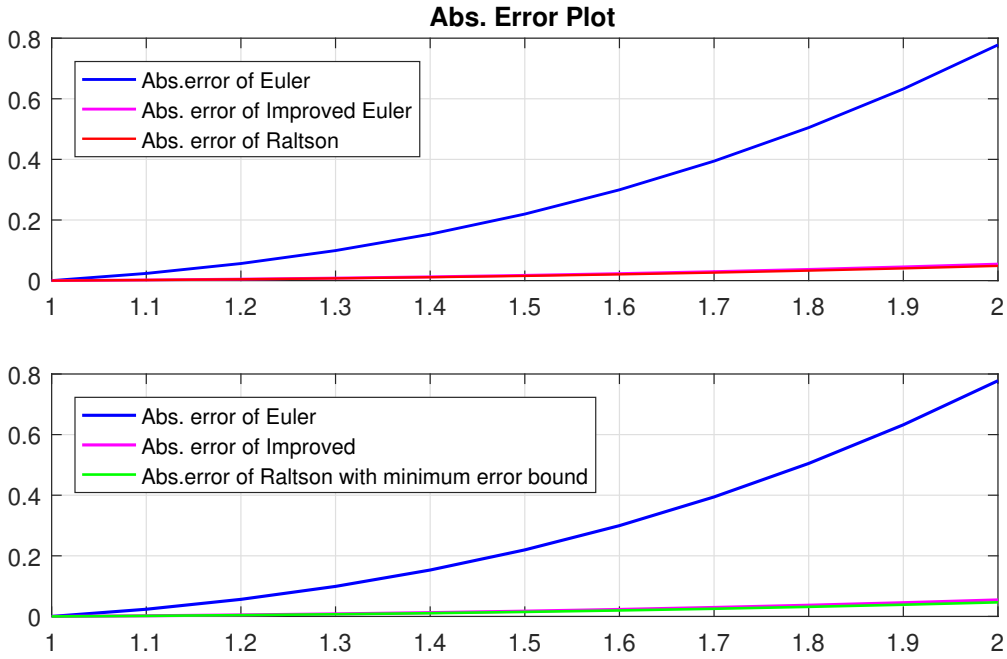

Fig. 11: Abs. error plot for Example 4

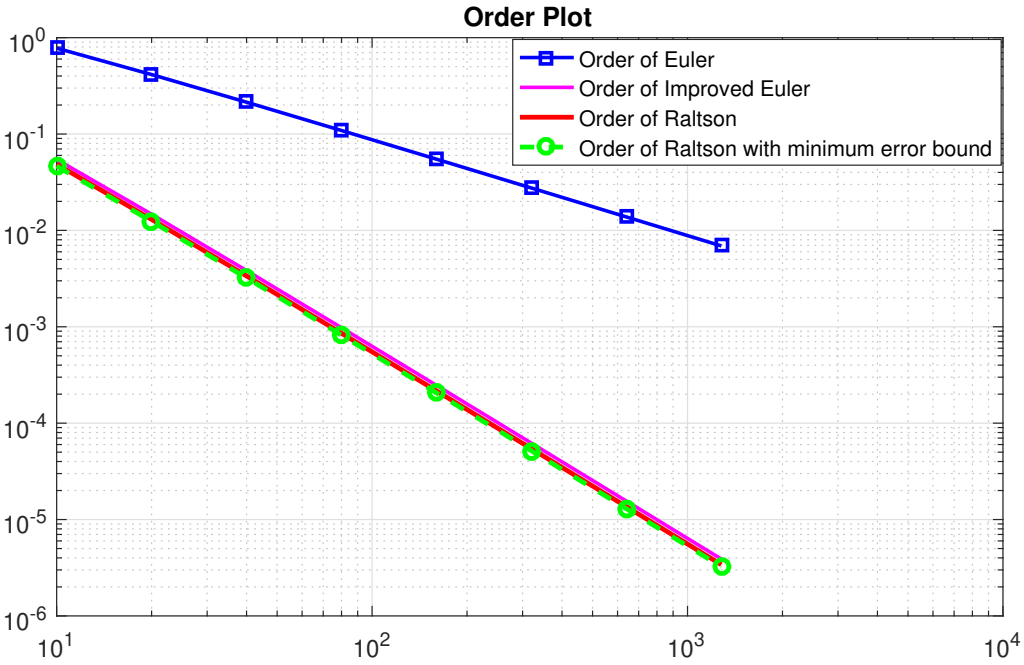

Fig. 12: Order graph of Example 4

5 Conclusion

Through out the present paper, we focused the two new technique RM and RME which is conventionally known as the Ralston method 1 and Ralston method 2 where both the method has quadratic convergence rate. The method presented in this paper is designed to compute the numerical solution of the IVP of FDEs with arbitrary order ρ, where $0 < \rho \leq 1$. To achieve this, we transform the Caputo fractional derivative into a classical fractional derivative of order one and apply the proposed numerical scheme to the revised FDEs. This transformation allows us to handle the fractional order derivatives in a way that is amenable to classical numerical techniques, enabling accurate approximation of the solutions. From our proposed scheme and numerical result, we recommend that is is more fast, and accurate compare to other linear convergence method like EM and quadratic convergence method like IEM, while our both methods has quadratic convergence rate. Also, we conclude that RME is fast and accurate compare to RM as RME has minimum local error bound in the comparison of all quadratic convergence method. We also conduct a comparative study between our proposed method and existing methods such as EM and IEM for the world growth model of population. Through this study, we aim to highlight the advantages of our proposed schemes, RM and RME, in solving FDEs.

The main advantages of our proposed schemes, RM and RME, can be summarized as follows:

- Our both method are more accurate, and comparatively fast comparing to other numerical technique like EM and IEM.
- Our work gives an idea to apply the analogously transform of the arbitrary FDEs into a classical ODE.
- The way of computation is quite well compare to other scheme and we can get more appropriate results by increasing the mesh points.

In conclusion, our proposed algorithms have demonstrated their effectiveness in obtaining numerical solutions for IVPs of FDEs. These methods have found accurate and faster.

References

[1] R. L. Bagley and P. J. Torvik, Fractional calculus in the transient analysis of viscoelastically damped structures, *AIAA J.* **23**(6), 918–925 (1985).
[2] F. Mainardi, *Fractional calculus and waves in linear viscoelasticity: an introduction to mathematical models*, World Scientific, 2010.
[3] J. T. Machado, V. Kiryakova and F. Mainardi, Recent history of fractional calculus, *Commun. Nonlin. Sci. Numer. Simul.* **16**(3), 1140–1153 (2011) .
[4] J. Sabatier, O. P. Agrawal and J. A. Tenreiro Machado , Advances in fractional calculus: theoretical developments and applications in physics and engineering, *Soc. Ind. Appl. Math.* **50**(3), 613-615 (2008).
[5] M. Ichise, Y. Nagayanagi and T. Kojima, An analog simulation of non-integer order transfer functions for analysis of electrode processes, *J. Elect. Chem. Inter. Electr.* **33**(2), 253–265 (1971).
[6] I. Podlubny, An introduction to fractional derivatives, fractional differential equations, to methods of their solution and some of their applications, *Math. Sci. Eng.* **198**, 1–340 (1999).
[7] R. Gorenflo and F. Mainardi, Fractional calculus: integral and differential equations of fractional order, arXiv preprint arXiv:0805.3823, 223–276 (2008).
[8] A. Loverro, *Fractional calculus: history, definitions and applications for the engineer*, Rapport technique, Univeristy of Notre Dame: Department of Aerospace and Mechanical Engineering, 1–28 (2004).
[9] R. P. Agarwal, V. Lakshmikantham and J. J. Nieto, On the concept of solution for fractional differential equations with uncertainty, *Nonlin. Anal. Theor. Meth. Appl.* **72**(6), 2859–2862 (2010) .
[10] R. P. Agarwal, D. O'Regan and S. Staněk, Positive solutions for Dirichlet problems of singular nonlinear fractional differential equations, *J. Math. Anal. Appl.* **371**(1), 57–68 (2010).
[11] A. Yakar and M. E. Koksal, Existence results for solutions of nonlinear fractional differential equations, *Abstr. Appl. Anal.* **2012**, (2012).
[12] K. S. Miller and B. Ross, *An introduction to the fractional calculus and fractional differential equations*, Wiley, 1993.
[13] I. Podlubny, *Fractional differential equations*, mathematics in science and engineering, Academic Press, New York **198**, 1999.
[14] J. He, Variational iteration method for delay differential equations, *Commun. Nonlin. Sci. Numer. Simul.* **2**(4), 235–236 (1997).
[15] J. H. He, Variational iteration method—some recent results and new interpretations, *J. Comput. Appl. Math.* **207**(1), 3–17 (2007).
[16] I. Hashim, O. Abdulaziz and S. Momani, Homotopy analysis method for fractional ivps, *Commun. Nonlin. Sci. Numer. Simul.* **14**(3), 674–684 (2009).
[17] G. Adomian, A review of the decomposition method in applied mathematics, *J. Math. Anal. Appl.* **135**(2), 501–544 (1988).
[18] H. Jafari and V. Daftardar-Gejji, Solving a system of nonlinear fractional differential equations using adomian decomposition, *J. Comput. Appl. Math.* **196**(2), 644–651 (2006).

[19] S. S. Ray and R. Bera, Analytical solution of the bagley torvik equation by adomian decomposition method, *Appl. Math. Comput.* **168**(1), 398–410 (2005).
[20] V. S. Ertürk and S. Momani, Solving systems of fractional differential equations using differential transform method, *J. Comput. Appl. Math.*, **215**(1), 142–151 (2008).
[21] Z. M. Odibat, S. Kumar, N. Shawagfeh, A. Alsaedi and T. Hayat, A study on the convergence conditions of generalized differential transform method, *Math. Meth. Appl. Sci.* **40**(1), 40–48 (2017).
[22] M. Khader and S. Kumar, An efficient computational method for solving a system of fdes via fractional finite difference method, *App. Appl. Math.* **14**(2), 32 (2019).
[23] K. Diethelm, N. J. Ford and A. D. Freed, Detailed error analysis for a fractional adams method, *Numer. Algorth.* **36**(1), 31–52 (2004).
[24] E. H. Doha, A. H. Bhrawy and S. S. Ezz-Eldien, A chebyshev spectral method based on operational matrix for initial and boundary value problems of fractional order, *Comput. Math. Appl.* **62**(5), 2364–2373 (2011).
[25] S. Kumar, P. K. Shaw, A.-H. Abdel-Aty and E. E. Mahmoud, A numerical study on fractional differential equation with population growth model, *Numer. Meth. Part. Differ. Equ.*, 1–22 (2020).
[26] S. S. Alzaid, P. K. Shaw and S. Kumar, A study of ralston's cubic convergence with the application of population growth model, *AIMS Math.* **7**(6), 11320–11344 (2022).
[27] S. S. Alzaid, P. K. Shaw and S. Kumar, A numerical study of fractional population growth and nuclear decay model, *AIMS Math.* **7**(6), 11417–11442 (2022).
[28] P. Tong, Y. Feng and H. Lv, Euler's method for fractional differential equations, *WSEAS Trans. Math.* **12**, 1146–1153 (2013).
[29] A. Jhinga and V. Daftardar-Gejji, A new finite-difference predictor-corrector method for fractional differential equations, *Appl. Math. Comput.* **336**, 418–432 (2018).
[30] S. Kumar, An analytical algorithm for nonlinear fractional fornberg–whitham equation arising in wave breaking based on a new iterative method, *Alexandria Eng. J.* **53**(1), 225–231 (2014).
[31] S. C. Chapra and R. P. Canale, *Numerical methods for engineers*, Boston: McGraw-Hill Higher Education, 2010.
[32] A. Ralston, Runge-kutta methods with minimum error bounds, *Math. Comput.* **16**(80), 431–437 (1962).
[33] A. Ralston and P. Rabinowitz, *A first course in numerical analysis*, Courier Corporation, 2001.
[34] J. A. Sandretto, Runge-kutta theory and constraint programming, *Reliable Comput.* **25**, 178–201 (2017).
[35] R. King, Runge-kutta methods with constrained minimum error bounds, *Math. Comput.* **20**(95), 386–391 (1966) .
[36] S. G. Samko, A. A. Kilbas and O. I. Marichev, *Fractional integrals and derivatives*, Gordon and Breach Science Publishers, Yverdon Yverdon-les-Bains, Switzerland **vol. 1**, 1993.
[37] A. A. Kilbas, H. M. Srivastava and J. J. Trujillo, *Theory and applications of fractional differential equations*, Elsevier, **Vol. 204**, 2006.
[38] K. Diethelm, *The analysis of fractional differential equations*: *An application-oriented exposition using differential operators of Caputo type*, Springer Science & Business Media, 2010.
[39] B. Shiri, G.-C. Wu and D. Baleanu, Terminal value problems for the nonlinear systems of fractional differential equations, *Appl. Numer. Math.* **170**, 162–178 (2021).
[40] M. B. Khan, H. M. Srivastava, P. O. Mohammed, D. Baleanu and T. M. Jawa, Fuzzy-interval inequalities for generalized convex fuzzy-interval-valued functions via fuzzy riemann integrals, *AIMS Math.* **7**(1), 1507–1535 (2022).
[41] G.-C. Wu, D.-Q. Zeng and D. Baleanu, Fractional impulsive differential equations: exact solutions, integral equations and short memory case, *Frac. Calc. Appl. Anal.* **22**(1), 180–192 (2019).
[42] A. Jajarmi, D. Baleanu, K. Z. Vahid, H. M. Pirouz and J. Asad, A new and general fractional lagrangian approach: A capacitor microphone case study, *Res. Phys.* **31**, 104950 (2021).
[43] D. Baleanu, M. H. Abadi, A. Jajarmi, K. Z. Vahid and J. Nieto, A new comparative study on the general fractional model of covid-19 with isolation and quarantine effects, *Alexandria Eng. J.* **61**(6), 4779–4791 (2022).
[44] K. Hosseini, M. Ilie, M. Mirzazadeh, A. Yusuf, T. A. Sulaiman, D. Baleanu and S. Salahshour, An effective computational method to deal with a time-fractional nonlinear water wave equation in the caputo sense, *Math. Comput. Simul.* **187**, 248–260 (2021).
[45] N. H. Luc, D. Baleanu, R. P. Agarwal and L. D. Long, Identifying the source function for time fractional diffusion with non-local in time conditions, *Comput. Appl. Math.* **40**(5), 1–21 (2021).
[46] P. A. Ravi, D. Baleanu, J. N. Juan and F. T. Delfim, A survey on fuzzy fractional differential and optimal control nonlocal evolution inclusions, *J. Comput. Appl. Math.* **339**, 3–29 (2018).
[47] K. Hosseini, A. Akbulut, D. Baleanu and S. Salahshour, The Sharma–Tasso–Olver–Burgers equation: its conservation laws and kink solitons, *Commun. Theor. Phys.* **74**(2), 025001 (2022).
[48] R. Almeida, N. R. Bastos and M. T. T. Monteiro, Modeling some real phenomena by fractional differential equations, *Math. Meth. Appl. Sci.* **39**(16), 4846–4855 (2016).
[49] Z. Odibat and S. Momani, An algorithm for the numerical solution of differential equations of fractional order, *J. Appl. Math. Infor.* **26**, 15–27 (2008).